P5.52 CO AND CH4 COLUMN RETRIEVAL FROM THE SCANNING HIGH RESOLUTION INTERFEROMETER SOUNDER (S-HIS)

Kenneth Vinson*, Henry Revercomb, H. Ben Howell, and Robert Knuteson
Space Science and Engineering Center, University of Wisconsin-Madison, Madison, WI

This study presents a new technique for the retrieval of CO and CH4 column amounts from high spectral resolution Fourier Transform Spectrometer (FTS) data. Results are presented from aircraft flights of the Scanning-High-resolution Interferometer Sounder (S-HIS). Case study results are presented from ER-2 underflights of the Terra satellite over controlled fires during the NASA SAFARI experiment in South Africa.

1. INTRODUCTION

In the ongoing effort to understand the composition, chemistry, and distribution of pollutants in the troposphere, it is important to have accurate measurements of gases such as Carbon Monoxide (CO) and Methane (CH4). Such measurements had been historically isolated and sometimes inaccurate. With the launch of the MOPITT instrument on board the NASA TERRA satellite in December 1999 there is now the potential for global CO and CH4 measurements. To help ensure accuracy of these measurements we have utilized data from an airborne Fourier Transform Spectrometer (FTS) to produce measurements of CO and CH4 optical depth along a flight path over a region of interest. These optical depths were obtained using an algorithm developed at the University of Wisconsin Space Science and Engineering Center (UW-SSEC) and applied to data gathered by the UW-SSEC Scanning HIS instrument (S-HIS) during a field experiment. The SAFARI-2000 mission in South Africa included flight paths coincident with overpasses of the NASA TERRA spacecraft and controlled fires. The MOPITT instrument on board the TERRA spacecraft is specifically designed to measure CO and CH4 column amounts. (Drummond, 1992) The optical depths obtained via the algorithm performed on S-HIS data may therefore be used in the validation of MOPITT CO and CH4 measurements as well as potential products of the NASA AIRS instrument on the EOS Aqua platform.

2. THEORETICAL DEVELOPMENT

In this section we present a treatment of the physical and mathematical aspects of the method used to derive optical depths. The primary assumptions are stated and justified.

The technique to be applied to the observations from the S-HIS instrument is one developed for the NASA SAFARI experiment to map CO distribution from fires.

* Corresponding Author Address: Kenneth H. Vinson, University of Wisconsin, Space Science and Engineering Center, 1225 W. Dayton St., Madison, WI 53706-1612; email: kenneth.vinson@ssec.wisc.edu

The method makes use of high spectral resolution emission lines observed by the S-HIS spectrometer to derive an optical depth using weak absorption lines. It is less sophisticated than a full profile retrieval approach, but is very useful for a survey result of localized events.

A ratio of on-line to off-line emission for selected lines of the gas of interest provides a measure of the gas amount. The selected wavenumbers are displayed in the table below.

Gas	On-line wn's	Off-line wn's
CO	2150.80	2151.77
	2154.667	2153.698
	2158.05	2159.02
	2158.52	2164.80
	2165.29	2166.75
	2165.77	2168.193
	2169.157	2170.126
	2172.54	2173.506
	2173.02	
CH4	1230.0	1230.96
	1240.62	1240.14
	1241.11	1241.59

The form of the equation to be used can easily be derived from a single-layer atmosphere approximation;

$$N_n^{Obs} = t_n \cdot N_n^{Surf} + N_n^{Atm} + t_n \cdot N_n^{\mathrm{Re}\,fl}$$

$$t_n = \exp[-t_\nu] \; and \; t = optical\ depth$$

$$Assume: N_n^{\mathrm{Re}\,fl} = 0; N_n^{Atm} = B_n(\overline{T_{Atm}})$$

where N^{Obs} is the S-HIS observed upwelling spectral radiance at an altitude of 20 km, t_ν is the atmospheric transmission for wavenumber ν, N^{Surf} is the emission from the surface, N^{Atm} is the atmospheric emission, N^{Refl} is the contribution from surface reflection, and B is the Planck emission function at a temperature T_A which approximates the mean atmospheric temperature. Neglecting the reflected radiance and substituting for the atmospheric emission leads to:

$$N_n^{Obs} \cong t_n \cdot N_n^{Surf} + B_n(\overline{T_{Atm}})$$

We then rearrange terms and split equation (2) into separate expressions for the on-line and off-line radiance.

$$t_{on} \cdot N_{on}^{Surf} = N_{on}^{Obs} - B_{on}(\overline{T_{Atm}})$$

$$t_{off} \cdot N_{off}^{Surf} = N_{off}^{Obs} - B_{off}(\overline{T_{Atm}})$$

We further assume that the surface emitted radiance is equal for both on-line and off-line spectral channels.

$$Assume: N_{on}^{Surf} = N_{off}^{Surf}$$

We may then divide equations (3) and (4) to obtain a ratio. We then use our earlier expression in equation (1) relating transmission to optical depth and substitute it,

$$Thus:$$

$$\frac{t_{on}}{t_{off}} = \frac{\exp(-t_{on})}{\exp(-t_{off})} = \frac{N_{on}^{Obs} - B_{on}(\overline{T_{Atm}})}{N_{off}^{Obs} - B_{off}(\overline{T_{Atm}})}$$

Take the natural log of both sides and the resulting expression becomes:

$$\Delta t = t_{on} - t_{off} = -\ln\left[\frac{N_{on}^{Obs} - B_{on}(\overline{T_{Atm}})}{N_{off}^{Obs} - B_{off}(\overline{T_{Atm}})}\right]$$

This result allows us to plot time series of changes in the optical depth of target gases. These results would be vulnerable to any dramatic change in the path distance between the emitter and the detector. The results therefore may be sensitive to conditions of heavy haze or cloud cover. Fortunately, there were also present on the ER-2 during the SAFARI experiment a cloud LIDAR system and an imaging system the MODIS Airborne Simulator (MAS). Data from these instruments were used to find clear sky regions on which to perform analysis of CO and CH4 optical depth.

3. DESCRIPTION OF EQUIPMENT

Scanning HIS Description

The Scanning HIS (S-HIS) is an advanced version of the HIS ER-2 instrument (Smith et al. 1987/89, Revercomb et al. 1988a), developed between 1996 and 1998 with the combined support of the US DOE, NASA, and the NPOESS Integrated Program Office. It has flown in seven field campaigns beginning in 1998 and has proven to be very dependable and effective. The continuous spectral coverage from 3.3 to 16.7 μm at 0.5 cm^{-1} resolution is illustrated in Figure 1 by a sample spectrum from the SAFARI-2000 mission in South Africa. This coverage is divided into three bands with separate detectors (two photoconductive HgCdTe and one InSb) to achieve the required noise performance. The bands use a common field stop to ensure accurate spatial co-alignment. The longwave band provides the primary information for temperature sounding for cloud phase and particle size. The midwave band provides the primary water vapor sounding information and further cloud property information. The shortwave band provides information on cloud reflectance and augments sounding information.

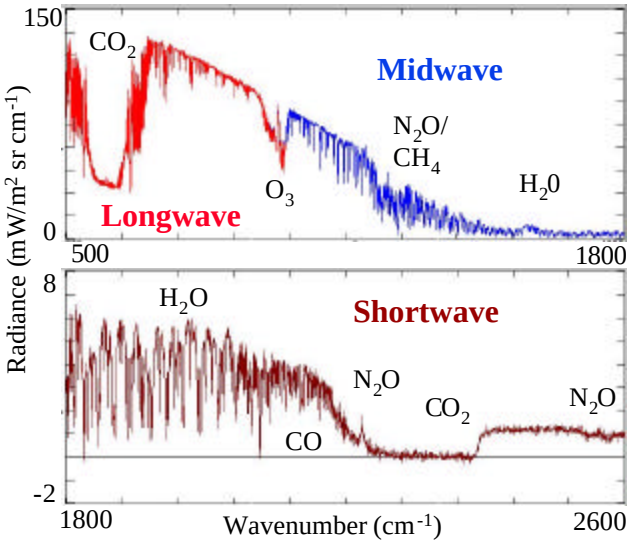

Figure 1. Sample Scanning HIS spectrum from NASA SAFARI-2000 mission. The three different spectral bands are color-coded. There is overlap between the longwave and the midwave band that is useful for diagnostics.

The optical design is very efficient, providing useful signal-to-noise performance from a single 0.5 second dwell time. This allows imaging with 2-3 km resolution to be accomplished by cross-track scanning. Onboard reference blackbodies are viewed as part of each cross-track scan, providing updated calibration information every 20-30 seconds. The rapid sampling frequency of the S-HIS allows cross-track imaging at 2 km resolution with a swath width on the ground of 30-40 km, as illustrated in Figure 2, or a nadir only mode with overlapping fields of view.

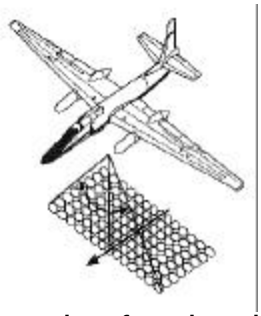

Figure 2. Illustration of swath angle and size subdivided into cells representing individual scans.

4. RESULTS

In this study we used data from several flights during the SAFARI field experiment when the NASA ER-2 was based in Pietersburg, South Africa. We focused our efforts on the flight of 7 September 2000. This was a daylight flight of the ER-2 which included three passes over a controlled fire set by SAFARI personnel. The times for the overpasses are summarized below:

First Overpass (North to South):
08:18:30 UTC to 08:23:36 UTC

Second Overpass (South to North):
08:41:30 UTC to 08:47:28 UTC

Third Overpass (North to South):
09:02:10 UTC to 09:08:30 UTC

The SHIS instrument was in nadir only mode for this flight obtaining a single spectrum from a 2 km field of view every 0.5 seconds along the aircraft flight path. Figure 3 is an image of the ER-2 flight track superimposed on a Meteosat image recorded very near the times of interest.

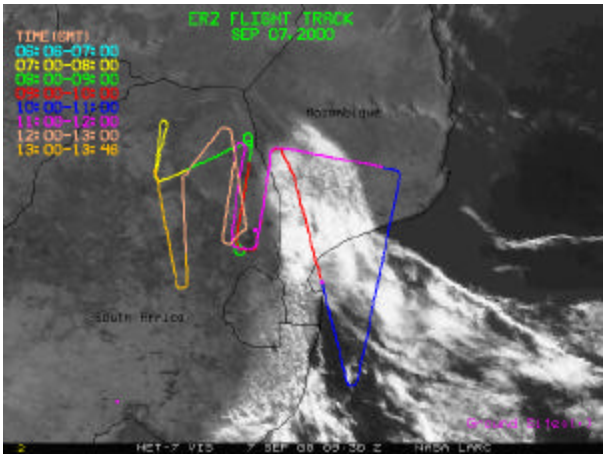

Figure 3. ER-2 flight track over Meteosat image.

It was expected that, as a primary combustion product, an increase in CO column density, and thus optical depth, would be observed during the data period when the ER-2 overflew the fire. The results obtained from our algorithm are consistent with this expectation. A significant peak in the CO optical depth is apparent in the SHIS data in each of the overpasses coincident in time with the controlled fire. This peak is also present in the brightness temperature for the nearby window region. The peak increase of the CO optical depth in the first overpass is ~40% over the background. The peak increase in the second and third overpasses is ~100% over the background level.

A verification of the cloud-free scene apparent in the MAS image of the target area can be observed in the optical depth of methane during the fire overpasses. The methane optical depth was not observed to vary significantly over all three overpasses of the fire site. This uniformity of methane optical depth can also be seen as an indicator that the mean atmospheric temperature assumed in our algorithm is sufficiently constant over the area of interest.

Figure 4 is a MODIS Airborne Simulator (MAS) view of the fire region during the first overpass (north to south). The target fire, with its attendant smoke plume, can be clearly observed near the center of the image. A larger, older burn scar can be seen near the top of the image. The SHIS observation path passes directly down the center of the MAS image. MAS images such as the one in Figure 4 were crucial to identifying the regions of interest present in SHIS SAFARI data.

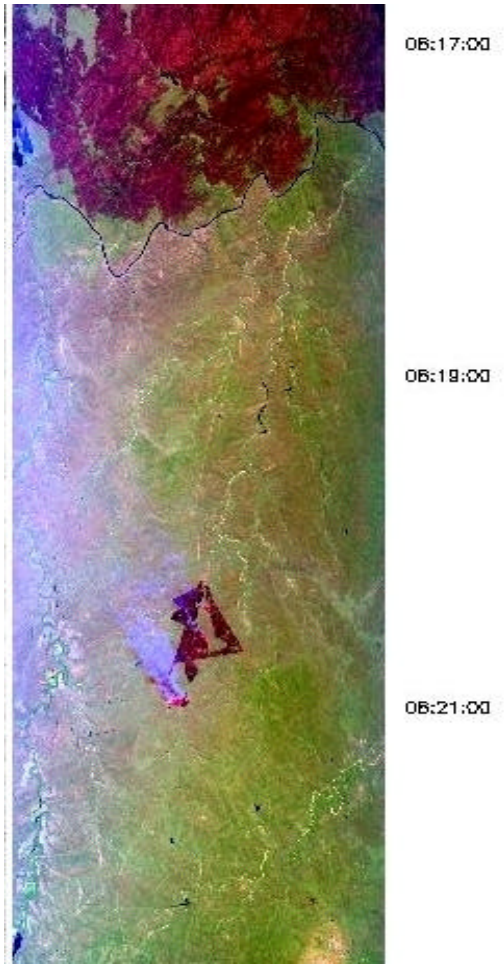

Figure 4. MAS view of fire region.

The results of the optical depth algorithm for CO and CH4 are plotted in Figure 5 with accompanying brightness temperatures for the 4 micron window region. In each of the three optical depth graphs CO is the top line and CH4 is the bottom line.

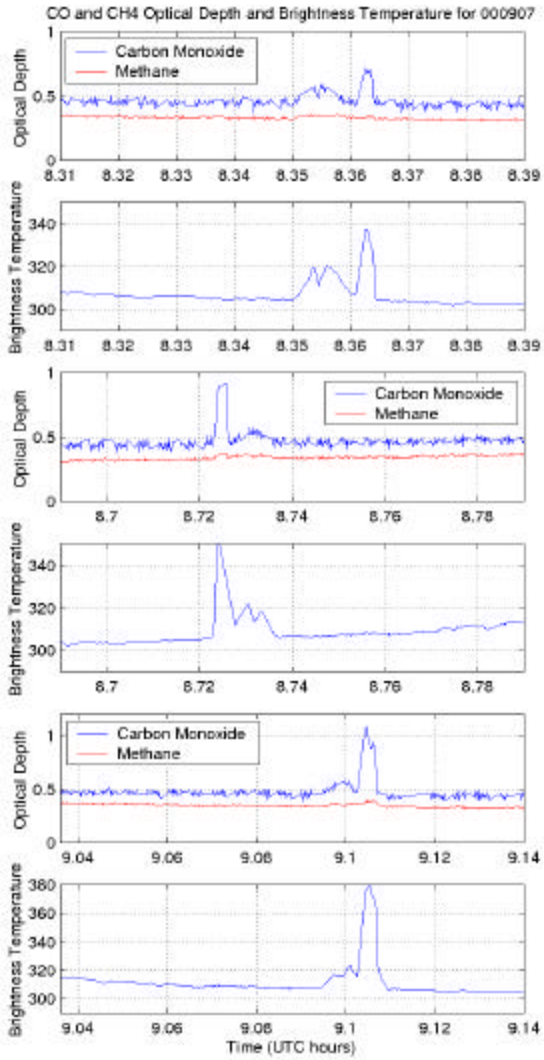

Figure 5. Derived optical depth results from S-HIS for three ER-2 overpasses of a controlled fire on 7 September 2000. Derived Carbon Monoxide and Methane optical depths are compared with the observed brightness temperature from the 4 micron region of S-HIS.

5. SUMMARY

A new technique is presented to derive trace gas column optical depth from high spectral resolution upwelling infrared emission spectra. The technique has been applied to accurately calibrated observations of the University of Wisconsin Scanning HIS instrument. Results have been presented showing a doubling of carbon monoxide optical depth over controlled fires observed by the S-HIS on the NASA ER-2 during the NASA SAFARI experiment. Future work includes validation of this technique and extension of it to the EOS AIRS instrument on the Aqua spacecraft platform.

6. REFERENCES

Drummond, J.R., 1992: Measurements of Pollution in the Troposphere (MOPITT), in *The Use of EOS for Studies of Atmospheric Physics*, J.C. Gille and G. Visconti, Eds., pp. 77-101, North-Holland, Amsterdam (1992)

King, M. D., W. P. Menzel, P. S. Grant, J. S. Myers, G. T. Arnold, S. E. Platnick, L. E. Gumley, S. C. Tsay, C. C. Moeller, M. Fitzgerald, K. S. Brown and F. G. Osterwisch, 1996: Airborne scanning spectrometer for remote sensing of cloud, aerosol, water vapor and surface properties. J. Atmos. Oceanic Technol., 13, 777-794.

McMillan, W.W., Strow, L.L., Smith, W.L., Revercomb, H.E., Huang, 1996: The detection of enhanced carbon monoxide abundances in remotely sensed infrared spectra of a forest fire smoke plume. Geophys. Res. Lett., 23(22):3199-3202.

Revercomb, H.E., D.D. LaPorte, W.L. Smith, H. Buijs, D.G. Murcray, F.J. Murcray, and L.A. Sromovsky, 1988a: High-Altitude Aircraft Measurements of Upwelling IR Radiance: Prelude to FTIR from Geosynchronous Satellite. Mikrochimica Acta [Wien], II, 439-444.

Revercomb, H.E., V.P. Walden, D.C. Tobin, J. Anderson, F.A. Best, N.C. Ciganovich, R.G. Dedecker, T. Dirkx, S.C. Ellington, R.K. Garcia, R. Herbsleb, R.O. Knuteson, D. LaPorte, D. McRae, and M. Werner, 1998: Recent results from two new aircraft-based Fourier transform interferometers: The Scanning High-resolution Interferometer Sounder and the NPOESS Atmospheric Sounder Testbed Interferometer, 8th International Workshop on Atmospheric Science from Space using Fourier Transform Spectrometry (ASSFTS), Toulouse, France, 16-18 November 1998.

Smith, W.L., H.M. Woolf, H.B. Howell, H.-L. Huang, and H.E. Revercomb, 1987/1989: The Simultaneous Retrieval of Atmospheric Temperature and Water Vapor Profiles - Application to Measurements with the High-resolution Interferometer Sounder (HIS). RSRM '87:Advances in Remote Sensing Retrieval Methods, A. Deepak, H. Fleming, J. Theon (Eds.). A. Deepak Publishing, Hampton, Virginia.